The University of Tehran Press

Pollution

Print ISSN: 2383-451X
Online ISSN: 2383-4501

https://jpoll.ut.ac.ir/

Dilution of a Single-Port Submerged Diffuser with Fixed Vanes

Ahmed Ashmawy[1] | M. H. Nasef[2] | Nouby M. Ghazaly[3,4]✉

1. National Water Research Center (NWRC), Hydraulics Research Institute (HRI), El-Qanater El-Khiriaya 13621, Egypt.
2. Department of Mechanical Power Engineering., Faculty of Engineering, Fayoum University, Fayoum 63514, Egypt.
3. Technical College, Imam Ja'afar Al-Sadiq University, Baghdad, Iraq.
4. Mechanical Eng. Dept., Faculty of Engineering, South Valley University, Qena-83523, Egypt.

Article Info

Article type:
Research Article

Article history:
Received: 24 March 2024
Revised: 6 August 2024
Accepted: 06 January 2025

Keywords:
Thermal pollution
Submerged diffuser
Temperature distribution
Propeller speed
Thermal discharge

ABSTRACT

Thermal pollution refers to the alteration of water properties caused by the use of water as a cooling fluid. This occurs when water is pulled from a water source, condensed to release heat, and then recirculated back into the water source as thermal discharge. The characteristics of thermal discharge dilution are influenced by factors such as jet momentum, buoyancy, turbulence-induced distribution, density stratification of the surrounding environment, configuration of water currents, presence of solid boundaries, and heat exchange at the surface. A single-port diffuser is used for the discharge of hot water. This study employed experimental methods to investigate the impact of fixed vanes on the thermal effluent dilution of a single-port submerged diffuser. The use of fixed vanes increases the dilution of a single-port submerged diffuser. Using fixed vans for H= 1, ΔT_m was reduced by 3.13%, 10.26%, and 2.74%, and ΔT_c was reduced by 15.66%, 17.86%, and 22.86%, respectively, for each flow ratio. For H= 2, ΔT_m decreased by 2.38%, 3.41%, and 4.48%, and ΔT_c decreased by 8.33%, 15%, and 16.67%, respectively, for each flow ratio. For H= 3, ΔT_m decreased by 2.86%, 2.22%, and 3.45%, and ΔT_c decreased by 5%, 29.41%, and 22.73%, respectively, for each flow ratio. In addition, increasing the Reynolds number ratio reduces the mixing zone and increases the dilution temperature.

Cite this article: Ashmawy, A., Nasef, M. H., & Ghazaly, N. M. (2025). Dilution of a Single-Port Submerged Diffuser with Fixed Vanes. *Pollution*, 11(1), 23-38.
https://doi.org/10.22059/poll.2024.374295.2305

 Publisher: The University of Tehran Press.
DOI: https://doi.org/10.22059/poll.2024.374295.2305

INTRODUCTION

Thermal pollution refers to the phenomenon of altering the properties of water by utilising it as a cooling fluid. This occurs when water is drawn from a source, condensed to release heat, and then recirculated back into the same water source, resulting in changes in the water's characteristics. The characteristics of thermal discharge dilution are influenced by factors such as jet momentum, buoyancy, turbulence-induced distribution, density stratification of the surrounding environment, configuration of water currents, presence of solid boundaries, and heat exchange at the surface. A single-port diffuser is a method employed to dispose of hot water. Numerous researchers have investigated the discharge of a single-port submerged diffuser. For instance, (Ashmawy et al., 2020) examined the mixing zone of a single-port submerged diffuser obstructed by a freely rotating propeller. They discovered that the propeller enhances the dispersion of hot water discharged from the diffuser. Additionally, they observed that increasing the distance of the propeller reduces the dilution of the hot water. Ahmad et al., (2012) conducted experiments to investigate the dispersion of a vertical negatively buoyant jet. They conducted five tests with different Froude numbers, and the flow was turbulent. The

*Corresponding Author Email: *noby_mehdi@ijsu.edu.iq*

equation of state for water was nearly linear. A jet is released in a vertical downwards direction into cold water. Thermocouples were employed to measure temperature fields, which were then utilised to investigate the characteristics of jet diffusion and dilution. Examinations of the temperature data revealed significant fluctuations in the vertical extent of jet penetration. The average and highest vertical jet diffusions derived from the temperature data in this investigation were in line with the findings of prior investigations.

Ahmad and Suzuki, (2016) conducted research on the concentrated discharge resulting from the desalination process. An investigation was conducted to observe the behaviour of vertical dense jets. This was done by releasing cold saline water in an upwards direction into a tank containing hot freshwater, all under normal environmental circumstances. The dilution was determined via thermocouples. Angelidis, (2001) created a numerical model to simulate the mixing of a submerged single jet that is discharged at an angle into still fluid. Further improvements were made to strengthen the model. The fundamental characteristics of the model included the preservation of thermal flow, the integration of turbulent heat flow across the jet, and the dependence of the entrainment coefficient on the local Richardson number. Chowdhury and Testik, (2014) conducted a comprehensive analysis on the dynamics of buoyant jet discharges from a single point buried in rivers, lakes, and coastal waters. This review focuses on gravity flows that occur both at the bottom boundary and at the water surface. The text summarises the artificial discharge processes that create two types of gravity currents and their impact on the surrounding hydro environment. The flow regime characteristics of these discharges before they transform into gravity currents and how they influence the dynamics of the gravity currents are also discussed. Additionally, it covers the dynamics of the gravity currents in calm receiving waters.

Economopoulou et al. (2003) conducted a study on the performance of outfalls with single buoyant plumes in flowing ambient sea water. They compared this performance with that of perpendicular line diffusers, taking into account all dilution mechanisms and their relationships. The graphs illustrate the comparative performance of outfalls equipped with single-port and perpendicular-line diffusers. The results indicate that outfalls with a single port exhibit superior performance to those with perpendicular line diffusers across a wide range of operating conditions. Huang et al., (1998) conducted a study on the initial dilution of a submerged single-port diffuser. Two semiempirical equations were formulated to calculate the centerline dilution and minimum surface dilution. These equations were generated using laboratory and field data, and the constants in the equations were determined. These equations are applicable for both vertical and horizontal jets. Huai and Fang (2006) conducted a numerical investigation on the efficiency of a submerged buoyant jet stopped by a disc to enhance the dilution rate in a stagnant uniform environment. They used a k–ε turbulence model for simulation. The model was validated using empirical data. The flow behind the disc was partitioned into three distinct regions: the wake region, the transitional zone, and the self-similarity region. The length of the wake zone varies depending on the flow and geometrical characteristics.

Jirka (2004) conducted a study on the mechanics of buoyant single jet flows in an uncontrolled ambient environment with uniform density and steady conditions. This study utilised a three-dimensional mathematical model based on the conservation of mass, momentum, buoyancy, and scalar quantities in turbulent jet flows. To enhance the accuracy of the model, an entrainment closure approach and a quadratic law turbulent drag force mechanism were employed. The model was validated through various means, including comparing it with fundamental experimental data for similar buoyant jet flows and comparing it with different types of nonequilibrium flows. Kim et al., (2004) investigated the mixing mechanisms of a buoyant jet released from a submerged single port. They employed a three-dimensional mathematical model to examine three different flow arrangements: co-flow, cross-flow, and oblique flow.

Experiments were conducted under different flow conditions to validate the model. The numerical and experimental results exhibited strong concordance, as the utilisation of both the jet integral and particle tracking approaches in hybrid modelling yielded favourable outcomes in approximating the vertical concentration distributions of co-flowing discharged jets. Kim and Cho (2006) conducted a study on a submerged jet of heated water that was discharged from a side outlet. They compared this with a surface discharge with cross flow. To do this, they used a three-dimensional numerical model. The experimental data were then used to verify the findings. Submerged discharge was determined to be more efficient than surface discharge. Kim and Seo (2002) conducted a study on a submerged jet of heated water discharged from a side outlet. They compared this submerged jet with a surface discharge using a three-dimensional numerical model. Experimental data were utilised to validate their findings. Submerged discharge was determined to be more efficient than surface discharge.

In their work, Marmorino et al., (2015) investigated the surface temperature distribution resulting from an upwards-discharging buoyant jet into water, specifically when it impinged on the water surface. An infrared camera was used to record the temperature distribution and the evolution of the turbulent-scale structures. During the process of receiving, the water remains relatively motionless, while the buoyant fluid travels in a nearly symmetrical manner. Both the temperature and velocity fields decrease gradually over a radial distance of a few tens of metres. If there is a water current, both the plume and thermal bands elongate in the downstream direction. Paik (2011) employed computational fluid dynamics to investigate the turbulent initial mixing of thermal discharge jets from a single-port diffuser in various cross flows. A three-dimensional model was utilised, and the governing equations were solved using a second-order accurate finite volume method. The model was validated using experimental data, and it was demonstrated that a CFD model can accurately simulate a thermal discharge jet in an artificial channel. This approach provides a reasonable and acceptable level of accuracy in predicting the turbulent initial mixing of buoyant jets under various cross-flow conditions. Stamou and Nikiforakis (2013) conducted a simulation of the thermal discharge from a thermal power station into the coastal seas in Mantoudi, Evia, Greece. This simulation of the discharged thermal jet utilised two models: one for predicting the close field using CorJet and the other for predicting the distant field using FLOW-3D. The model was validated using experimental data, and its predictions were compared with those of the far-field CORMIX model. It was determined that the integrated model is more accurate than a single model for both near-field and far-field predictions. Tang et al., (2008) employed computational fluid dynamics (CFD) in a three-dimensional manner to model the mixing occurring in the close vicinity of thermal discharge. The simulation of buoyancy effects utilised an algebraic mixing length model with a Richardson number correction for turbulence closure. A second-order accurate approach was employed to solve the governing equations. Validation was conducted, and the results were found to be in excellent agreement with the experimental measurements. A comparison was conducted between a model used to simulate the mixing of thermal discharge from single-port and multiport diffusers and two existing models. The results obtained from applying two commonly used empirical mixing zone models indicate that the results are highly similar. Therefore, the model can be utilised to accurately predict mixing in the immediate vicinity of thermal discharge. Wen-xin et al. (2006) conducted a study on thermal buoyant jets discharged from submerged circular jets. They used computational fluid dynamics and a three-dimensional numerical simulation with the buoyancy-realizable k-ε model. This study focused on analysing the plume length, centreline trajectory, and temperature dilutions of the jets. The numerical findings were compared to the experimental data to validate the model. It was determined that the model successfully predicted the velocity distribution and temperature dilutions, making it a valuable tool for forecasting the behaviour of wall buoyant jets.

Yazdi and Marvasti (2010) employed the finite volume flow solver of NASIR software to

simulate the mixing process resulting from thermal discharge. The simulation findings were validated by comparing the experimental temperature field with the results obtained from a three-dimensional numerical solution. The researchers determined that the simulation results offer valuable insights into the environmental consequences of a submerged thermal jet and the potential impacts of natural circulations near the water outlet of the power station. Zeng and Huai (2008) employed an experimental approach to validate a numerical method for predicting the behaviour of a round buoyant jet in cross flow with varying velocity ratios. The velocity ratio was identified as the most influential characteristic for thermal discharging in a cross flow. The trends were accurately forecasted. The numerical and experimental results exhibited a high degree of concordance. This work utilised computational fluid dynamics, specifically a three-dimensional numerical simulation using the buoyancy and RNG - k-ε model, to examine thermal buoyant jets released from a submerged port. Experiments were performed at various velocity ratios to validate the theoretical analysis. The numerical and experimental results exhibited a high degree of concordance. Researchers have determined that employing the finite technique with the RNG-k-ε model is an effective approach for simulating spherical heated buoyant jets released from a submerged port in a flowing environment. Ibrahim et al. (2023) employed two-dimensional simulation, using (k- ε) as the turbulence model and the physical characteristics of open channel flow, to study submerged deep port diffusers with changing inclination angles and developed a mathematical equation to estimate the temperature in open channels based on the study parameters.

The aim of this research is to investigate thermal effluent dilution using a single-port submerged diffuser with fixed vanes to help reduce the negative effect of thermal effluent on water bodies. This study will alter the following parameters: measurement of the water depth above the diffuser and comparison of the Reynolds number ratios using an experimental technique. Most of the previous researches were taken into consideration Froude number larger than (1) which is not common in open channel flow (usually lower than one in open channel flow). In this research Froude number is lower than one, also taking into account the effect of Reynolds number on thermal effluent dilution using a single-port submerged diffuser.

MATERIALS AND METHODS

Procedure and methodology of the experiment:

An experimental flume was constructed at the Hydraulic Research Institute to investigate the dilution of a single port submerged diffuser when obstructed by fixed vanes. Fig. (1) depicts a schematic representation of the flume and the devices required for conducting the experimental measurements, as in (Ashmawy et al., 2020). The physical model (i.e., flume) consists of 3 parts (i.e., the flume entrance, body, and exit) with two pumps. Flume entrance: The flume entrance receives water from the main pump through a receiving tank (i.e., 3 m long, 0.5 m wide and 1.5 m high). There is a 0.4 m high weir at the entrance to dissipate the energy and a gabion filled with stones to avoid flow disturbance.

Flume body: The flume main body is an 18 m long and 2 m wide concrete bed flume. The flume conveys water from the intake canal (i.e., linked to the river).

Flume exit: The flume exit consists of a manually revolving steel tailgate to control the water level in the flume. The revolving tailgate is fixed on the flume bed.

Pumps: There are 2 pumps to impel water to the model, where the main pump impels cold water under a head (h) of 10 m and provides a discharge of 0.07 m^3/s. On the other hand, the secondary pump impels hot water under a head (h) of 15 m and provides a discharge of 0.007 m3/s. The physical model is equipped with an electric water heater to represent the thermal power station as a source of heated water. The electric water heater power is 120 KW. Its capacity is 2 m^3. It consists of three groups of heaters (i.e., each group consists of nine heaters). A thermostat controlled the temperature of the water. The physical model is equipped with the

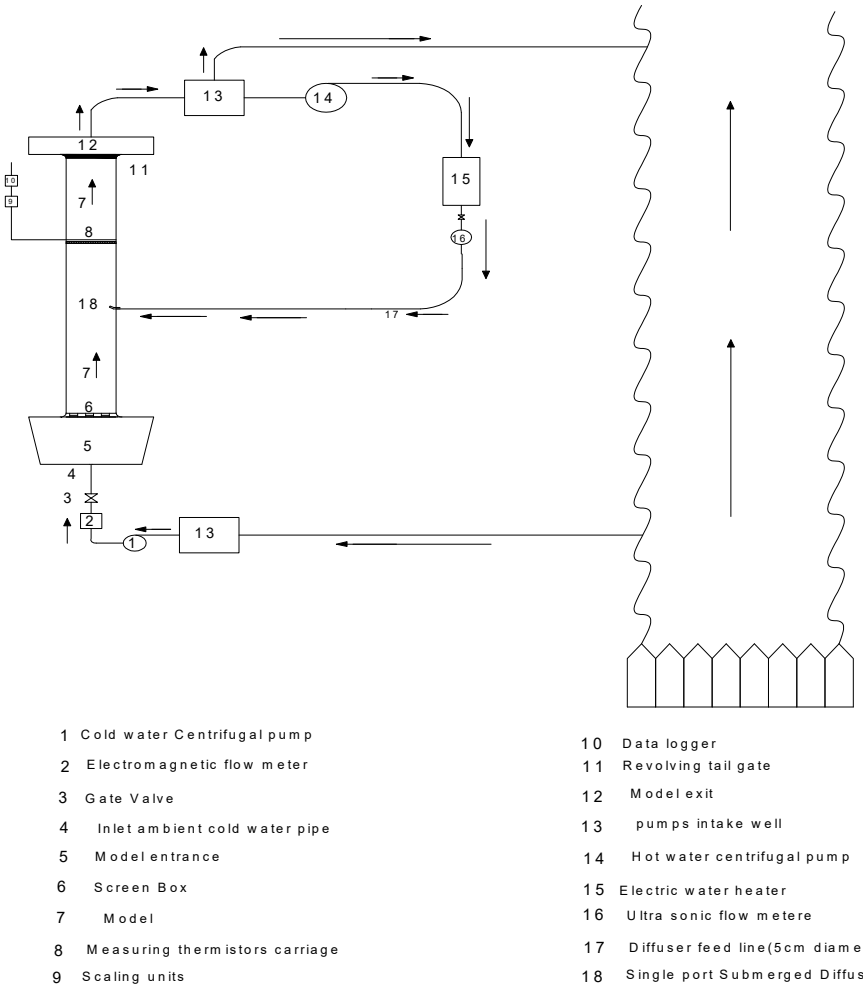

Fig. 1. Schematic diagram of the experimental setup.

following measuring devices:

Ultrasonic flow meter: This meter measures the hot water discharge flow rate. It is mounted on a 2-inch steel pipe that conveys hot water to the flume. The velocity range of the ultrasonic flow meter is 0-12 m/s. Its accuracy is 1%. It was calibrated before and during the experimental tests to ensure that the measurements were accurate**.** The electromagnetic flowmeter was used to measure the cold-water discharge flow rate. It has a diameter of 6 inches. The measuring range of the velocity is 0.1-10 m/s. Its accuracy is 0.5%. It was calibrated before and during the experimental tests to ensure that the measurements were accurate.

Thermistors (i.e., 23 thermistors) measure the temperature distribution along the width of the model. Their measuring range was 0-90 °C. Their accuracy is ± 0.1 °C. They were calibrated before and during the experimental tests.

Connectors connected to thermistors (each handles 10 thermistors).

Data acquisition (i.e., 40 channels) converts the analogue signal from each thermistor to a digital reading and record it. They were all mounted on a movable carriage to measure the temperature over the entire model. Fig. (2) presents the temperature measurement locations

Experimental work was accomplished to examine the dilution of single port submerged diffusers with guide vanes discharging hot water in ambient water. The diffuser outlet is a 0.05 m diameter pipe inclined at an angle of 30° in the horizontal direction and 20° in the vertical

direction. The difference between the ambient water discharge and hot water discharge was Δ T =10,8 C°. The surface temperature was measured across the model using thermistors. Fig. 3 shows a single-port diffuser with guide vanes. The test procedure was as follows:

The model water level is set to the required value by using a tailgate mounted at the end of the model. The cold water was discharged into the flume, and the discharge was adjusted by an electromagnetic flowmeter. The electric water heater heats the water to the required temperature. The flow rate into the heater was adjusted by an ultrasonic flow meter. The temperature distribution is measured upstream and downstream of a single-port diffuser. The temperature distribution in the model is measured by thermistors after steady-state conditions are reached. The temperature readings were recorded at the selected positions for each experiment. The data were acquired by measuring the temperature 3 times at each position every 9 minutes. Three flow rate ratios (Q_r) between hot water and ambient water flow were considered (0.2, 0.4, and

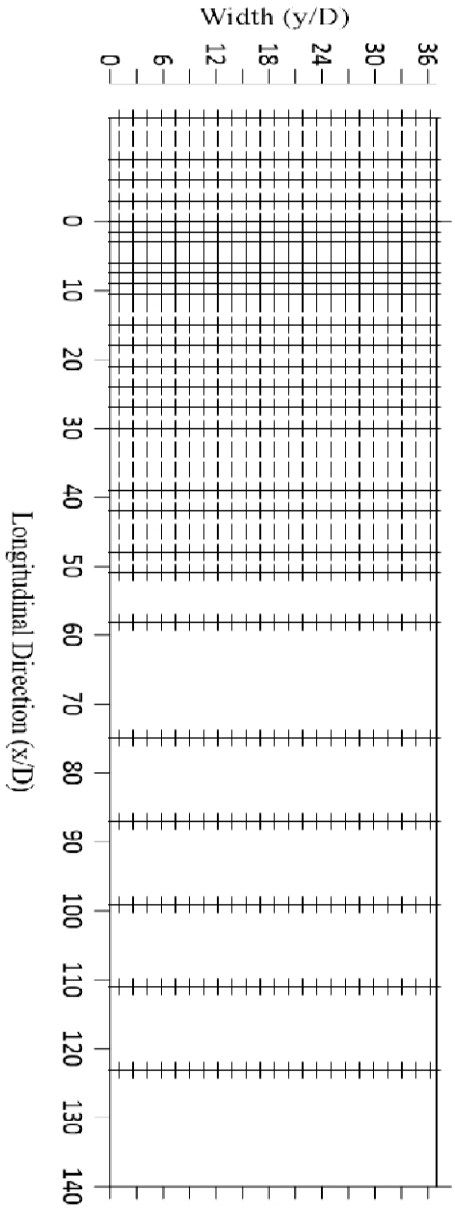

Fig. 2. Temperature measurement locations.

Fig. 3. Single-port submerged diffuser obstructed by fixed vanes.

0.67). The temperature difference was plotted as ($\Delta T_f/\Delta T$). Three flow ratios and three water depth ratios above the diffuser (H=1, 2, and 3) were considered.

First, a single-port submerged diffuser was tested without any modifications. Then, the single-port submerged diffuser was obstructed by fixed vanes. This was achieved to study the impact of fixed vanes on the mixing zone at Δ T =10 °C under three water depth ratios above the diffuser (i.e., H=1, 2, and 3) with three flow ratios. Fig. 3 shows a single port submerged diffuser obstructed by fixed vanes.

RESULTS AND DISCUSSION

The SPSD was analysed without any modifications. The analysis was performed for the case where the temperature difference between the ambient water and hot water discharged was Δ T =10 °C. In addition, the analysis was carried out on the results of three water depth ratios above the diffuser (i.e., H = 1, 2 and 3) under the effect of varying the flow ratio (i.e., Qr =0.2, 0.4, 0.67). Moreover, analysis was carried out for the case where the height above the diffuser was H=1 and Δ T = 10 °C under three flow ratios (i.e., Q_r = 0.2, 0.4, and 0.67) with 2 Reynolds number ratios (Re_r). Based on the analysis results, graphs were reproduced and presented, where the temperature difference ratios were designated $\Delta T_f/\Delta T$ in the longitudinal direction and transverse direction. Among these graphs are the following: Fig. 4 presents the dilution of the plume center temperature ratios for H=1.

Furthermore, analysis was carried out for the case where the height above the diffuser was H=2 and Δ T = 10 °C under three flow ratios (i.e., Q_r = 0.2, 0.4, and 0.67) with 2 Reynolds number ratios (Re_r). Based on the analysis results, graphs were reproduced and presented, where the temperature difference ratios were designated $\Delta T_f/\Delta T$ in the longitudinal direction and transverse direction. Fig. 5 shows the dilutions of the plume center temperature ratios for H=2.

Likewise, analysis was carried out for the case of investigating a height above the diffuser of H=3, Δ T = 10 °C under three flow ratios (i.e., Q_r = 0.2, 0.4, and 0.67) with 2 Reynolds number ratios (Re_r). Based on the analysis results, graphs were reproduced and presented, where the temperature difference ratios were designated $\Delta T_f/\Delta T$ in the longitudinal direction and

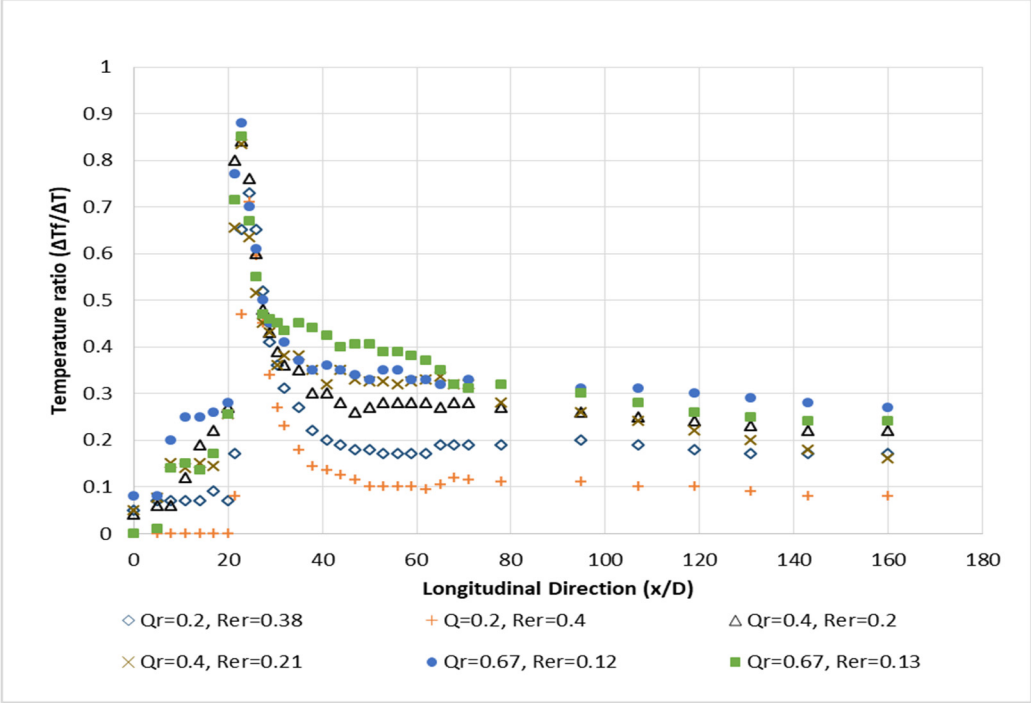

Fig. 4. Dilution of the plume center temperature ratios for H=1.

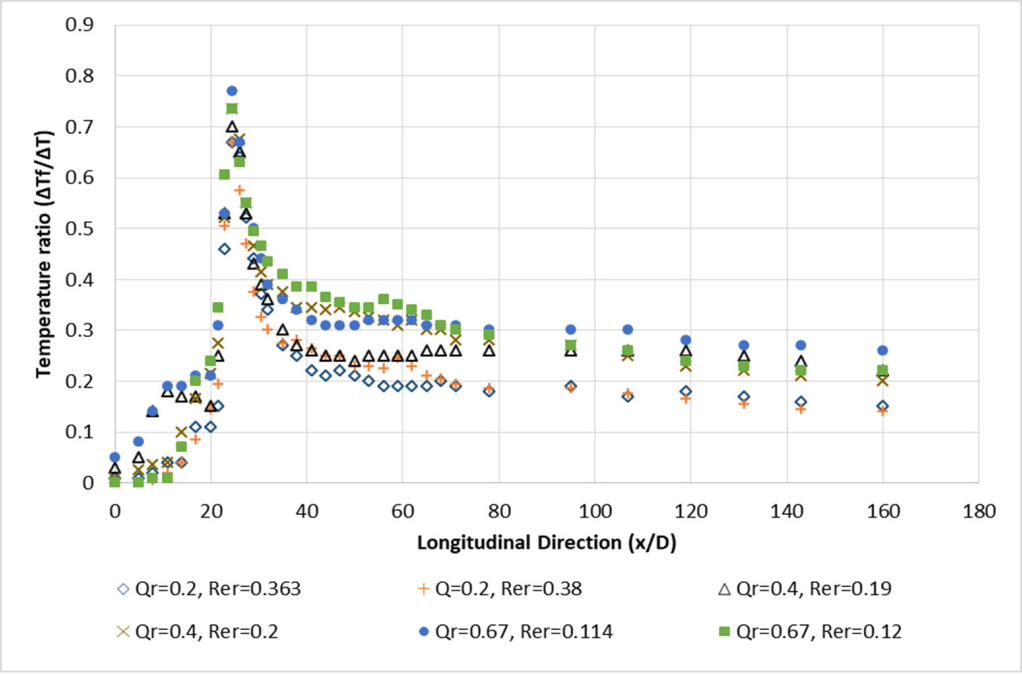

Fig. 5. Dilution of the plume center temperature ratios for H=2.

transverse direction. Fig. 6 shows the dilutions of the plume center temperature ratios for H=3.

Based on the executed analysis, the plume center temperature ratios (ΔT_m) and average temperature ratio at the end of the measurements (ΔT_e) are listed and presented in Table 1 for flow ratios (Q_r = 0.2, 0.4, and 0.67) at Reynolds number ratios (Re_r).

Based on the analysis of the measurement results, the following conclusions were drawn:

Increasing Re_r for different H and Q_r reduced ΔT_m and ΔT_e at H= 1, where ΔT_m decreased by

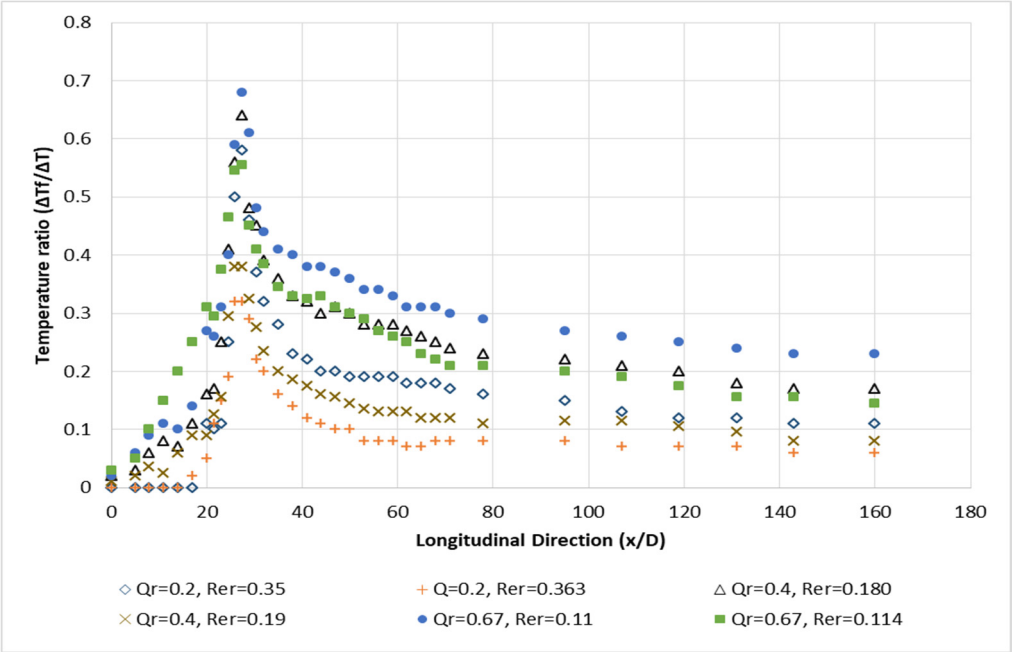

Fig. 6. Dilution of the plume center temperature ratios for H=3.

Table 1. ΔTm and ΔTe for the diffusers without modifications

H	Q_r	Re_{r1}	ΔT_{m1}	ΔT_{e1}	Re_{r2}	ΔT_{m2}	ΔT_{e2}	ΔT_{mc} (%)	ΔTe_c (%)
1	0.2	0.38	0.73	0.166	0.4	0.71	0.137	-2.74	-17.47
	0.4	0.2	0.84	0.28	0.21	0.83	0.22	-1.19	-21.43
	0.67	0.12	0.88	0.35	0.13	0.86	0.31	-2.27	-11.43
2	0.2	0.363	0.67	0.12	0.38	0.65	0.1	-2.99	-16.67
	0.4	0.19	0.7	0.2	0.2	0.69	0.19	-1.43	-5.00
	0.67	0.114	0.9	0.3	0.12	0.73	0.27	-18.89	-10.00
3	0.2	0.35	0.58	0.1	0.363	0.32	0.07	-44.83	-30.00
	0.4	0.18	0.64	0.17	0.19	0.39	0.09	-40.63	-47.06
	0.67	0.11	0.68	0.22	0.114	0.55	0.18	-19.12	-18.18

2.74%, 1.19%, and 2.27%, while ΔT_e decreased by 17.47%, 21.43%, and 11.43%, respectively, for each flow ratio. For H= 2, ΔT_m was reduced by 2.99%, 1.43%, and 18.89%, and ΔT_e was reduced by 16.67%, 5%, and 10%, respectively, for each flow ratio. For H= 3, ΔT_m decreased by 44.83%, 40.63%, and 19.12%, and ΔT_e decreased by 30%, 47.06%, and 18.18%, respectively, for each flow ratio. Increasing the Reynolds number ratio reduces the mixing zone and increases the dilution temperature

Increasing H from (1 to 2) with Re_{rl} reduced ΔT_m and ΔT_e. At H= 2, ΔT_m decreased by 8.22%, 16.67%, and 2.27%, and ΔT_e decreased by 27.71%, 28.57%, and 14.29%, respectively, for each flow ratio. Increasing H from (1 to 3) with Re_{rl} reduced ΔT_m by 20.55%, 23.81%, and 22.73% and ΔT_e by 39.76%, 39.29%, and 37.14%, respectively, for each flow ratio. Increasing H above the diffuser increases the dilution temperature and reduces the mixing zone.

Single-port submerged diffuser obstructed by fixed vanes:

The analysis was performed for the case where the temperature difference between the ambient water and hot water discharged was Δ T =10 °C. In addition, the analysis was carried out on the results of three water depth ratios above the diffuser (i.e., H = 1, 2 and 3) under the effect of

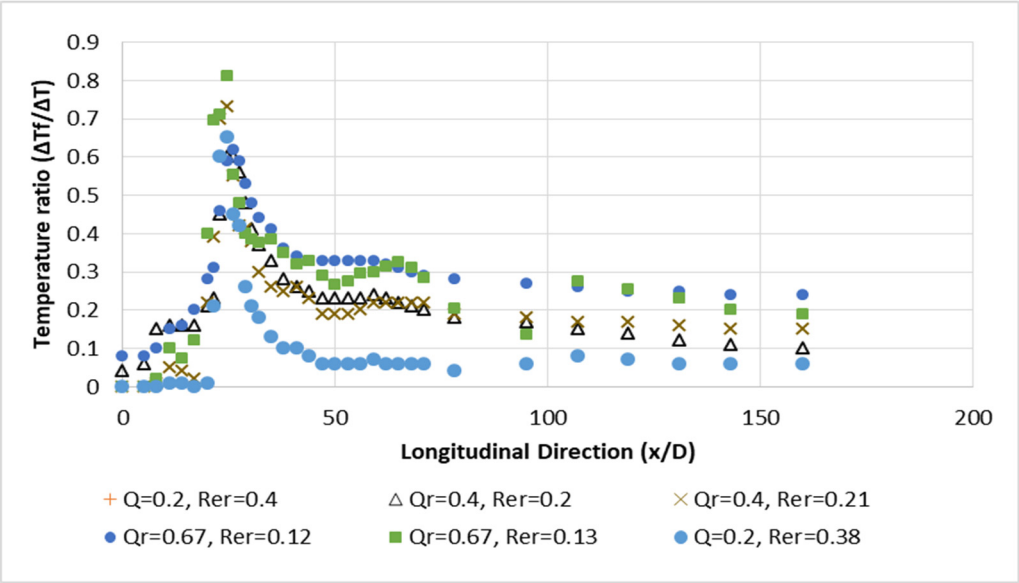

Fig. 7. Dilution of the plume center temperature ratios for the single-port submerged diffuser obstructed by fixed vanes at H=1.

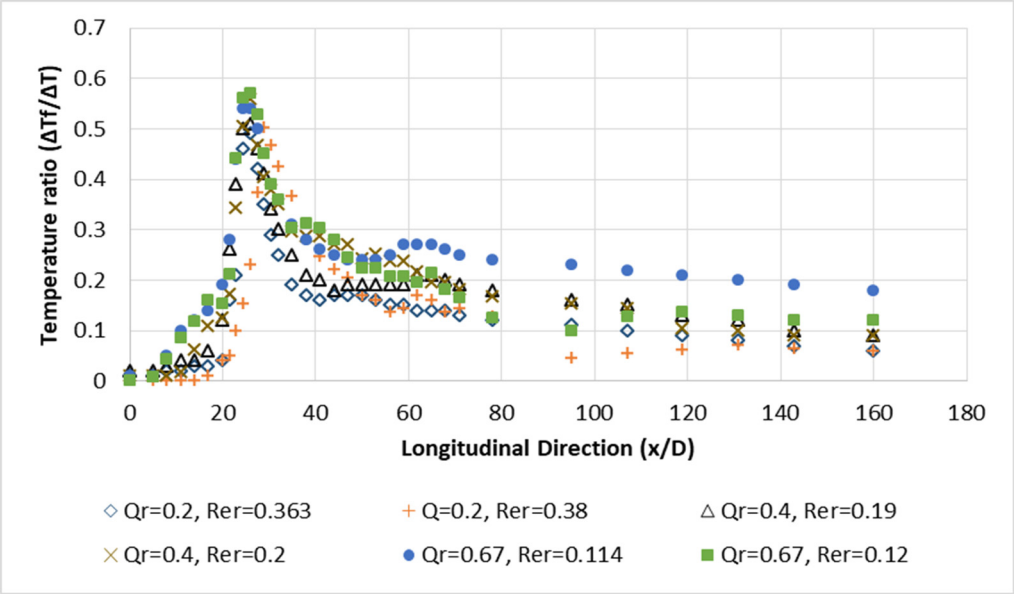

Fig. 8. Dilution of the plume center temperature ratios for the single-port submerged diffuser obstructed by fixed vanes at H=2.

varying the flow ratio (i.e., Qr =0.2, 0.4, 0.67). Moreover, analysis was carried out for the case where the height above the diffuser was H=1 and Δ T = 10 °C under three flow ratios (i.e., Q_r = 0.2, 0.4, and 0.67) with 2 Reynolds number ratios (Re_r). Based on the analysis results, graphs were reproduced and presented, where the temperature difference ratios were designated $\Delta T_f / \Delta T$ in the longitudinal direction and transverse direction. Fig. 7 shows the dilution of the plume center temperature ratios for the single-port submerged diffuser obstructed by fixed vanes at H=1. Additionally, Fig. 8 shows the dilution of the plume center temperature ratios for the single-port submerged diffuser obstructed by fixed vanes at H=2. Fig. 9 Dilution of the plume center

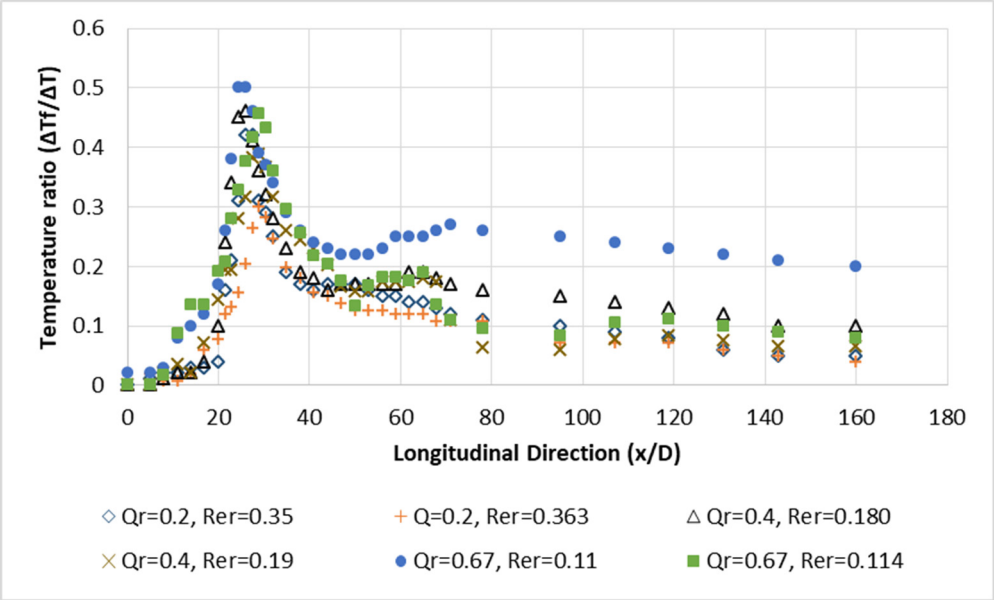

Fig. 9. Dilution of the plume center temperature ratios for the single-port submerged diffuser obstructed by fixed vanes at H=3.

Table 2. Comparison between (ΔT_{mp}) and (ΔT_{ep}) at Re_r for a single-port submerged diffuser obstructed by fixed vanes

H	Q_r	Re_r	ΔT_m fixed vanes	ΔT_m	ΔT_{mc} (%)	ΔT_e fixed vanes	ΔT_e	ΔT_{ec} (%)
1	0.2	0.4	0.68	0.71	4.23	0.116	0.137	15.33
	0.4	0.21	0.77	0.83	7.23	0.17	0.22	22.73
	0.67	0.13	0.83	0.86	3.49	0.2	0.31	35.48
2	0.2	0.38	0.51	0.65	21.54	0.09	0.1	10.00
	0.4	0.2	0.59	0.69	14.49	0.14	0.19	26.32
	0.67	0.12	0.6	0.73	17.81	0.21	0.27	22.22
3	0.2	0.363	0.31	0.32	3.12	0.065	0.07	7.14
	0.4	0.19	0.35	0.39	10.25	0.089	0.09	1.11
	0.67	0.114	0.53	0.55	3.64	0.16	0.18	11.11

Table 3. Comparison between ΔT_{mp} and ΔT_{ep} at Re_r for a single-port submerged diffuser obstructed by fixed vanes

H	Q_r	Re_r	ΔT_m fixed vanes	ΔT_m	ΔT_{mc} (%)	ΔT_e fixed vanes	ΔT_e	ΔT_{ec} (%)
1	0.2	0.38	0.71	0.73	3.13	0.14	0.166	15.66
	0.4	0.2	0.82	0.84	10.26	0.23	0.28	17.86
	0.67	0.12	0.85	0.88	2.74	0.27	0.35	22.86
2	0.2	0.363	0.64	0.67	2.38	0.11	0.12	8.33
	0.4	0.19	0.68	0.7	3.41	0.17	0.2	15.00
	0.67	0.114	0.88	0.9	4.48	0.25	0.3	16.67
3	0.2	0.35	0.56	0.58	2.86	0.095	0.1	5.00
	0.4	0.18	0.63	0.64	2.22	0.12	0.17	29.41
	0.67	0.11	0.65	0.68	3.45	0.17	0.22	22.73

temperature ratios for the single-port submerged diffuser obstructed by fixed vanes at H=3.

Tables 2 and 3 show a comparison between the plume center temperature ratio (ΔT_m) and the average temperature ratio at the end of the measurements (ΔT_e) for various flow ratios (Q_r = 0.2,

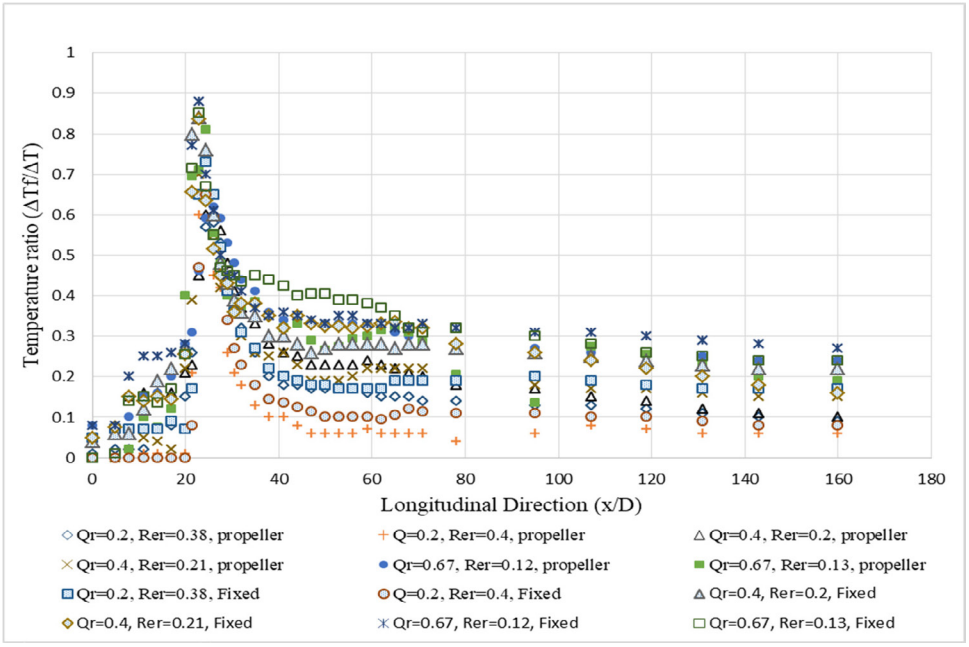

Fig. 10. Dilution of the plume center temperature ratios for a single-port submerged diffuser obstructed by fixed vanes and a propeller at H=1.

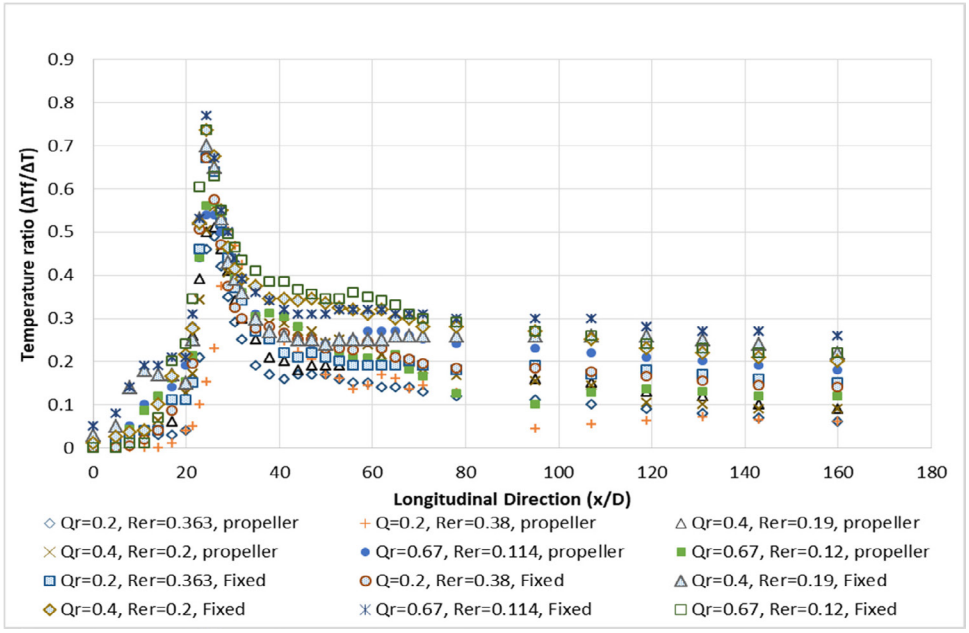

Fig. 11. Dilution of the plume center temperature ratios for a single-port submerged diffuser obstructed by fixed vanes and a propeller at H=2.

0.4, and 0.67) and Reynolds number ratios (Re_r) for a single-port submerged diffuser obstructed by fixed vanes.

For H= 1, ΔT_m decreased by 3.13%, 10.26%, and 2.74%, and ΔT_e decreased by 15.66%, 17.86%, and 22.86%, respectively, for each flow ratio. For H= 2, ΔT_m decreased by 2.38%, 3.41%, and 4.48%, and ΔT_e decreased by 8.33%, 15%, and 16.67%, respectively, for each flow ratio. For H= 3, ΔT_m decreased by 2.86%, 2.22%, and 3.45%, and ΔT_e decreased by 5%, 29.41%, and 22.73%, respectively, for each flow ratio. The investigation revealed a clear relationship: when fixed vanes were used on a single-port submerged diffuser, the temperature dilution

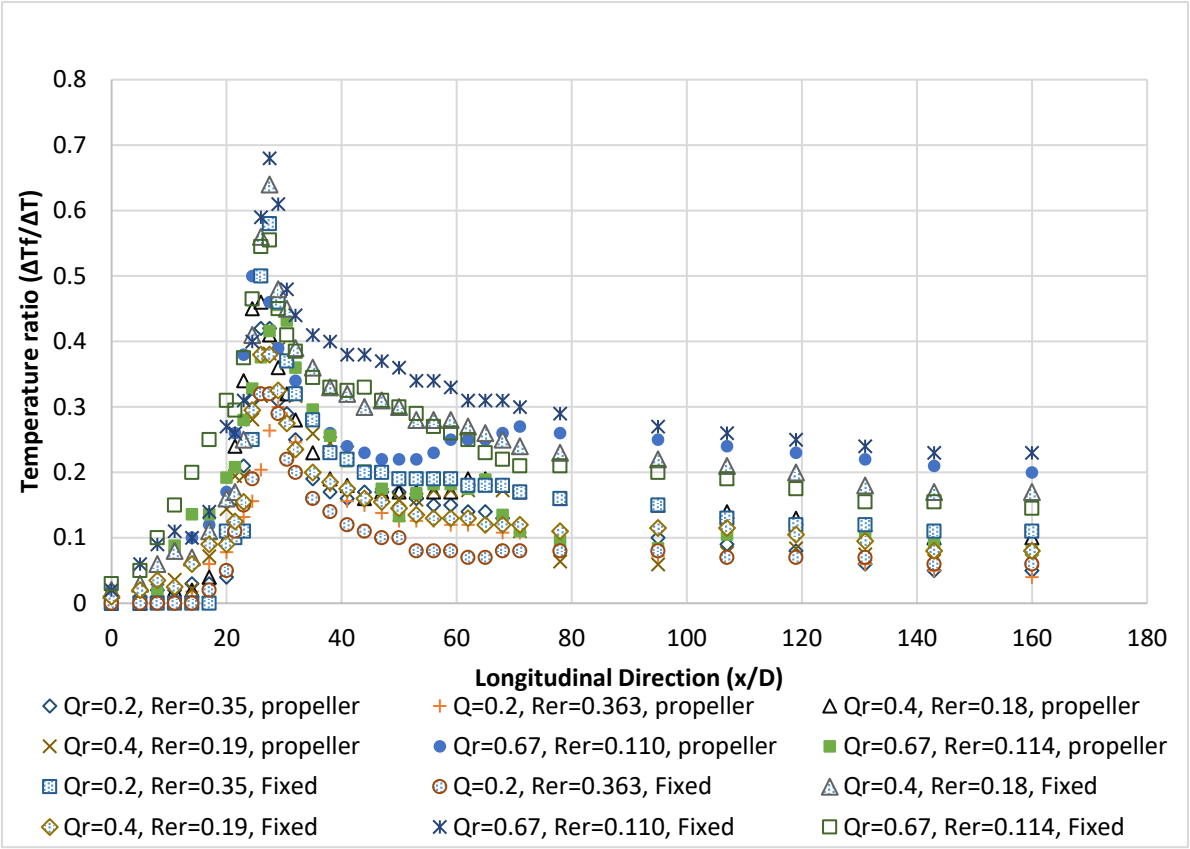

Fig. 12. Dilution of the plume center temperature ratios for a single-port submerged diffuser obstructed by fixed vanes and a propeller at H=3.

increased, and the mixing zone decreased. A comparison was made with (Ashmawy et al. 2020), Fig. 10 dilution of plume center temperature ratios for a single-port submerged diffuser obstructed by fixed vanes and a propeller at H=1. Fig. 11 shows the dilution of the plume center temperature ratios for the single-port submerged diffuser obstructed by fixed vanes and the propeller at H=2. Fig. 12 Dilution of the plume center temperature ratios for a single-port submerged diffuser obstructed by fixed vanes and a propeller at H=3. The comparison was made at the same Reynolds number ratio and water depth above the diffuser. From the comparison, it was found that using a rotating impeller increased the dilution of hot water and thus reduced the mixing zone.

CONCLUSION

The present research investigated the dilution of a single-port submerged diffuser with fixed vanes. The water depth above the diffuser was measured, and the Reynolds number ratios were compared via an experimental technique. Increasing the Reynolds number ratio reduces the mixing zone and increases the dilution temperature. Additionally, increasing H above the diffuser increases the temperature dilution and reduces the mixing zone. In addition, using fixed vanes on a single-port submerged diffuser increases the temperature dilution, and using fixed vanes on a single-port submerged diffuser reduces the mixing zone. Using single-port submerged diffuser with fixed vanes to help reduce the negative effect of thermal effluent on water bodies, by increases the temperature dilution, and using fixed vanes on a single-port submerged diffuser reduces the mixing zone.

GRANT SUPPORT DETAILS

The present research did not receive any financial support.

CONFLICT OF INTEREST

The authors declare that there is not any conflict of interests regarding the publication of this manuscript. In addition, the ethical issues, including plagiarism, informed consent, misconduct, data fabrication and/ or falsification, double publication and/or submission, and redundancy has been completely observed by the authors.

LIFE SCIENCE REPORTING

No life science threat was practiced in this research.

DATA AVAILABILITY

All data are provided in the manuscript.

NOMENCLATURE

Abbreviation	Quantity	Units
D	Diameter of diffuser	m
F_r	Froude number	
g	Acceleration gravity	m/s^2
h	Water-depth above diffuser	m
H	Water depth above diffuser to diffuser diameter ratio	
k	Turbulent kinetic-energy	
l	Distance between diffuser exit and propeller	m
L	Propeller distance to diffuser diameter ratio	
Q_H	Hot water discharge	m^3/s
Q_C	Ambient water discharge	m^3/s
Q_r	Hot water discharge to ambient water discharge ratio	
Re_H	Hot water discharge Reynolds number	Re_H
Re_C	Ambient water discharge Reynolds number	Re_C
Re_r	Ambient water discharge Reynolds number to hot water discharge Reynolds number ratio	Re_r
$\Delta T \Delta T$	Hot water and cold water temperature difference	^oC
ΔT_f	Difference between cold water temperature and temperature at any point	^oC
ΔT_m ($\Delta T_{fM}/\Delta T \Delta T_{fM}/\Delta T$)	Plume-center temperature ratio	
ΔT_e ($\sum(\Delta T_f/\Delta T)/n$ $\sum(\Delta T_f/\Delta T)/n$)	Average-temperature ratio	
ΔT_{mc}	Change in plume-center temperature ratio	
ΔT_{ec}	Change in Average-temperature ratio	

u	Velocity	m/s
ρ	Density	kg/m^3
w	Experimental model Width	m
x	Experimental model-longitudinal direction	m
Plume center Temperature	Plume maximum temperature	^oC
Average temperature	The sum of temperatures divided by the number of temperatures	^oC
SPSD	Single port submerged diffuser	

REFERENCES

Ahmad, N., & Baddour, R. E. (2012). Dilution and penetration of vertical negatively buoyant thermal jets. *Journal of Hydraulic Engineering*, *138*(10), 850–857.

Ahmad, N., & Suzuki, T. (2016). Study of dilution, height, and lateral spread of vertical dense jets in marine shallow water. *Water Science & Technology*, *73*(12), 2986–2997.

Angelidis P.B. (2001). A Numerical Model for The Mixing of an Inclined Submerged Heated Plane Water Jet in Calm fluid. *International Journal of Heat and Mass Transfer*, volume, 45, pp. 2567–2575.

Ashmawy, A., Aboelnasr, M., El-Ghorab, E. A., Hashim, M., & Abotaleb, H. (2020). Dilution of single port submerged diffuser clogged by a free rotating propeller. *American Journal of Engineering and Applied Sciences*, *13*(2), 182–190.

Chowdhury M.R., and Testik F.Y. (2014). A review of gravity currents formed by submerged single-port discharges in inland and coastal waters. *Environ Fluid Mech*., volume 14, pp. 265–293.

Economopoulou, M. A., Economopoulou, A. A., & Economopoulos, A. P. (2003). Sensitivity Analysis and Comparative Performance of Outfalls with Single Buoyant Plumes. *Journal of Environmental Engineering*, *129*(2), 169–178.

Huai, W., & Fang, S. (2006). Numerical simulation of obstructed round buoyant jets in a static uniform ambient. *Journal of Hydraulic Engineering*, *132*(4), 428–431.

Huang, H., Fergen, R. E., Proni, J. R., & Tsai, J. J. (1998). Initial dilution equations for Buoyancy-Dominated jets in current. *Journal of Hydraulic Engineering*, *124*(1), 105–108.

Jirka G.H. (2004). Integral Model for Turbulent Buoyant Jets in Unbounded Stratified Flows. Part I: Single Round Jet. *Environmental Fluid Mechanics*, Volume 4, pp.1–56.

Kim D.G., and Cho H.Y. (2006). Modeling the buoyant flow of heated water discharged from surface and submerged side outfalls in shallow and deep water with a cross flow. *Environ Fluid Mech.*, volume 6, pp. 501–518.

Kim, J. K., Savulescu, L., & Smith, R. (2001). Design of cooling systems for effluent temperature reduction. *Chemical Engineering Science*, *56*(5), 1811–1830.

Kim, Y. D., Seo, I. W., Kang, S. W., & Oh, B. C. (2002). Jet Integral–Particle Tracking Hybrid model for single buoyant jets. *Journal of Hydraulic Engineering*, *128*(8), 753–760.

Ibrahim, M., Ashmawy, A., Dalia, M., & Refaey, M. A. (2023). Numerical investigation of the effect of hot-water outlet inclination angle on the temperature dilution in open channel flow. *Ain Shams Engineering Journal*, *14*(12), 102234.

Marmorino, G., Savelyev, I., & Smith, G. B. (2014). Surface thermal structure in a shallow-water, vertical discharge from a coastal power plant. *Environmental Fluid Mechanics*, *15*(1), 207–229.

Paik J. (2011). Numerical Simulation of Thermal Discharges in Crossflow . *IEEE 3rd International Conference on Communication Software and Networks*, Xi'an, China, pp. 328-332.

Stamou A.I., and Nikiforakis I.K. (2013). Integrated modelling of single port, steady-state thermal discharges in unstratified coastal waters. *Environ Fluid Mech.,* volume 13, pp. 309–336.

Tang H.S., Paik J., Sotiropoulos F., and Khangaonkar T. (2008). Three-Dimensional Numerical Modeling of Initial Mixing of Thermal Discharges at Real-Life Configurations. *Journal of Hydraulic Engineering,* Volume 134, pp. 1210-1224.

Wen-xin H. and Shen-guang F. (2006). Rounded flowing states of obstructed buoyant jet. *Applied Mathematics and Mechanics*, *27*(8), 1133–1139.

Huai, W., Fang, S., & Dai, H. (2006). Behavior of obstructed square buoyant vertical jets in static

ambient (I)—verification of mathematical model and numerical method. *Applied Mathematics and Mechanics*, *27*(5), 645–652.

Yazdi S.S. R., and Marvasti S.S. (2010). Depth average simulation of thermal mixing mechanism of a power-plant in the coastal region. *Second International Symposium on Environmental Engineering*, January 19-21, Tehran, Iran.

Zeng, Y., & Huai, W. (2008). Characteristics of round thermal discharging in a flowing environment. *Journal of Hydro-environment Research*, *2*(3), 164–171.